ETS-RT - 2006-001

ON FORCE CONTROL OF PNEUMATIC ACTUATOR SUBJECT TO A POSITION TRACKING AND A FRICTION ESTIMATION BASED ON LUGRE MODEL

KARIM KHAYATI, PASCAL BIGRAS
AND LOUIS-A. DESSAINT

ETS-RT - 2006-001

ON FORCE CONTROL OF PNEUMATIC ACTUATOR SUBJECT TO A POSITION TRACKING AND A FRICTION ESTIMATION BASED ON LUGRE MODEL

CONTRÔLE DE FORCE D'UN ACTIONNEUR PNEUMATIQUE SOUMIS À UN SUIVI DE TRAJECTOIRE DE DÉPLACEMENT ET UNE ETIMATION DE LA FORCE DE FROTTEMENT BASÉE SUR LE MODÈLE DE LUGRE

ETS TECHNICAL REPORT

KARIM KHAYATI, PASCAL BIGRAS
Département de génie de la production automatisée

LOUIS-A. DESSAINT
Département de génie électrique

ÉCOLE DE TECHNOLOGIE SUPÉRIEURE
UNIVERSITÉ DE QUÉBEC

MONTRÉAL, 19 JUIN 2006

ETS-RT - 2006-001

ON FORCE CONTROL OF PNEUMATIC ACTUATOR SUBJECT TO A POSITION TRACKING AND A FRICTION ESTIMATION BASED ON LUGRE MODEL

KARIM KHAYATI, PASCAL BIGRAS
Département de génie de la production automatisée
ÉCOLE DE TECHNOLOGIE SUPÉRIEURE

LOUIS-A. DESSAINT
Département de génie électrique
ÉCOLE DE TECHNOLOGIE SUPÉRIEURE

Electronic version of this technical report is available on the École de technologie supérieure web site (http://www.etsmtl.ca).

In order to request a paper copy, please contact :

Service de la bibliothèque
École de technologie supérieure
1100, rue Notre-Dame Ouest
Montréal (Québec)
H3C 1K3

Phone : (514) 396-8946
Fax : (514) 396-8633
Email : biblio@etsmtl.ca

ISBN 2-921145-60-X

Legal Deposit : Bibliothèque et Archives nationales du Québec, 2006
Legal Deposit : Library and Archives Canada, 2006

CONTRÔLE DE FORCE D'UN ACTIONNEUR PNEUMATIQUE SOUMIS À UN SUIVI DE TRAJECTOIRE DE DÉPLACEMENT ET UNE ETIMATION DE LA FORCE DE FROTTEMENT BASÉE SUR LE MODÈLE DE LUGRE

KARIM KHAYATI, PASCAL BIGRAS ET LOUIS-A. DESSAINT

SOMMAIRE

Les systèmes d'actionneurs pneumatiques sont caractérisés par leur structure de modèle généralement complexe mise à l'épreuve d'une dynamique fortement non linéaire (due à la compressibilité de l'air et au facteur de frottement très élevé), une structure (géométrique, mécanique et thermodynamique) très perplexe de la valve et des incertitudes (variations thermodynamiques) des paramètres du modèle non linéaire (Lai et al., 1989 ; Richer and Hurmuzlu, 2000 ; Khayati et al., 2003). La dynamique de force et les grandeurs cinétiques (comme la vitesse) de ces dispositifs sont affectées par la charge externe. Tout cet *imbroglio* de facteurs affecte en effet la performance des servo-systèmes pneumatiques; en terme de précision (erreur de poursuite) et de rapidité (temps de réponse, cycle limite, *etc.*). En plus, la complexité du couplage de force/position de tel système rend la procédure de contrôle de force crucialement importante (*i.e.* non négligeable); surtout lorsqu'il est question de résolution du problème de contrôle de position et de compensation de frottement de ces dispositifs. Une manière rudimentaire pour réduire l'influence de la compressibilité du gaz est d'augmenter la pression (Kain and Wartelle, 1973 ; Mc Cloy and Martin, 1973). Cette solution reste très onéreuse. Elle vaudrait une augmentation des coûts d'installation et de maintenance. En effet, il faudrait redimensionner toute l'installation (ajout de compresseur, extension dans les conduites de transmission, *etc.*). Tout cela explique pourquoi les actionneurs pneumatiques sont sou-

vent abandonnés, lorsqu'ils sont sujet à des commandes rapides et précises; contrairement aux actionneurs électriques et hydrauliques par exemple.

Dans ce rapport, nous développons une stratégie de commande de force, qui est considérée comme une étape indispensable (à cause de la complexité de couplage qui se trouve entre la dynamique de force et celle de position dans ce cas). Ici, nous abordons la question de contrôle de force d'un actionneur pneumatique dans un contexte particulier où l'évolution des grandeurs cinétiques (position et vitesse) est considérée non forcément bornées. Cette technique de commande de force est accommodée pour le développement de la commande de position et de la compensation de frottement du système d'actionneur pneumatique. En effet, la dynamique de contrôle de pression dans les chambres du vérin est considérée indépendante de celle de position du piston et de la charge. Les perturbations causées par le mouvement de la partie mécanique ne peuvent pas être considérées bornées *a priori*. Ce travail représente une continuité (ou un complément) de certaines contributions précédemment élaborées en rapport avec ce sujet. Nous avons déjà développé une technique de commande linéarisante et de synthèse de retour d'état linéaire pour réaliser un schéma de contrôle de force d'un actionneur pneumatique. La dynamique d'erreur du système en boucle fermée est affectée dans ce cas, par des signaux exogènes de perturbations bornées (Khayati et al., 2002a, 2004).

Le système que nous considérons consiste en un cylindre pneumatique à volume variable dont la pression permet de manipuler le piston amovible en force et/ou position. Une servo-valve (valve proportionnelle à tiroir) est utilisée pour contrôler l'écoulement d'air

comprimé et, par conséquent, la pression dans les chambres du cylindre. La force motrice appliquée sur l'assemblage {piston + tige + charge}, sous l'effet des pressions d'air que subit le piston de chaque côté, est exprimée par un modèle dynamique non linéaire à paramètres incertains (Khayati et al., 2002a, 2003, 2004 ; Bigras, 2005). Dans (Khayati et al., 2002b,a, 2003), nous avons déjà élaborée une étude exhaustive (caractéristiques, propriétés, conditions et modélisations) des systèmes d'actionneurs pneumatiques. La position du tiroir de la valve (grandeur mécanique de la valve) est supposée proportionnelle à la tension d'excitation (grandeur électrique). La dynamique de la structure mécanique de la valve est considérée, *a priori*, négligeable devant la constante de temps de l'ensemble du système (Khayati et al., 2002a, 2004).

L'objectif de la commande proposée est d'assurer un suivi de la force pneumatique selon une forme spécifique qui varie dans le temps. Nous procédons d'abord par une annulation de la plupart des non linéarités et des termes non bornés connues du système. Ensuite, nous développons une combinaison d'un contrôleur linéaire de type PI (Khayati et al., 2004) et d'un compensateur non linéaire *atténuant* (Khalil, 2002), pour stabiliser la dynamique d'erreur de force en boucle fermée et limiter l'effet des perturbations dont les limites des variations sont *a priori* inconnues ou non forcément bornées. Comme dans (Khayati et al., 2002a, 2004), la synthèse des gains de la commande linéaire est basée sur le principe de placement de pôle robuste dans une région de stabilité, exprimé en termes de LMIs. Elle répond aux spécifications désirées du système en boucle fermée en terme de marge de stabilité exponentielle (*i.e.* temps de réponse), d'amortissement (*i.e.* dépassement maximum) et de dynamique (*i.e.* fréquences des modes oscillatoires) du

contrôleur et du système en boucle fermée, et en tenant-compte des incertitudes paramétriques structurées et bornées (Scherer et al., 1997 ; Chilali et al., 1999).

Admettons en outre que, dans le contexte de positionnement du vérin pneumatique sous frottement, la force de référence est, par définition, une fonction variable de la vitesse et est une combinaison de la force de frottement estimée. En particulier, en accord avec la modélisation de la force de frottement et son estimation, nous pouvons écrire la fonction dérivée du signal de référence comme une combinaison de termes continus qui représentent une fonction d'approximation de la dérivée du signal de référence et d'autres discontinus pour décrire son erreur d'approximation, par un paramètre incertain, qui inclut l'aspect de discontinuité de la force de frottement au voisinage de la vitesse nulle. Le terme, de commande non linéaire continue, proposé est utilisé pour atténuer ou compenser l'effet des termes exogènes qui agissent sur la dynamique d'erreur de force en boucle fermée. L'approche de la commande non linéaire atténuante associée à ce terme présente une version légèrement modifiée de la technique équivalente introduite dans (Khalil, 2002); qui garantit la robustesse par rapport à un paramètre multiplicatif incertain qui existe dans le schéma dynamique discuté ici.

Le résultat de ce schéma adéquatement choisi est très utile pour le traitement du problème de contrôle de mouvement de l'actionneur sous frottement. Il permet de garantir une solution bornée de la dynamique de force. Un *Experimentum* est développé pour illustrer l'efficacité de cette stratégie particulière de contrôle de force étudiée ici. Le signal d'entrée, *i.e.* le déplacement du tiroir de la valve qui est proportionnel à la tension

d'excitation de la valve, et les différentes mesures, les signaux de sortie, sont respectivement envoyé et acquis par un ordinateur via une carte d'acquisition. L'algorithme de contrôle est implémenté en utilisant les applications *XPC-Simulink* et *Real-Time-Workshop* dans le logiciel MATLAB©. Le schéma-bloc implémenté dans *Simulink* est transformé en code *C*, sur un ordinateur hôte équipé avec *Windows-OS*. Un dispositif exécutable est ensuite construit dans un ordinateur cible équipé de *XPC-OS*. Les deux ordinateurs hôte et cible utilisent une communication de *TCP/IP*. La synthèse des différentes LMIs est résolue initialement dans *LMI Toolbox* de MATLAB© (Gahinet et al., 1995). À travers les résultats obtenus, nous notons que la force mesurée tend rapidement vers la force désirée grâce à la contrainte de placement de pôle. L'effort de commande est acceptable même en présence d'incertitude de paramètres parfois variant brutalement.

Pour récapituler, nous notons que la combinaison de la technique de commande atténuante avec la formulation LMI du sous-problème linéaire constitue la contribution dans le présent travail. Il s'agit en outre d'un travail intermédiaire dans la stratégie générale de contrôle des systèmes pneumatiques étudiée dans cette application.

ON FORCE CONTROL OF PNEUMATIC ACTUATOR SUBJECT TO A POSITION TRACKING AND A FRICTION ESTIMATION BASED ON LUGRE MODEL

KARIM KHAYATI, PASCAL BIGRAS AND LOUIS-A. DESSAINT

ABSTRACT

The purpose of this paper is to develop an accurate closed-loop force controller design for a pneumatic actuator, submitted to a positioning control strategy using a LuGre-friction-model-based friction compensation. Since an analytical nonlinear structure, which is dependently affine on parameter uncertainties, generically characterizes pneumatic plants, a feedback linearization design is proposed to cancel out most of the resulting nonlinearities. We then propose a linear state feedback control and an additive nonlinear action to robustly bound the force-error dynamics. These devices are required to handle the further parametric uncertainties and exogenous unbounded disturbances that will arise on the deduced structure. The linear control gains are designed within robust closed-loop pole clustering using the linear matrix inequality (LMI) framework. Finally, various experimental results illustrate the validity of the approach.

TABLE OF CONTENTS

LIST OF TABLES

LIST OF FIGURES

1 INTRODUCTION

The usage of pneumatic actuators has been of growing demand for automation and mobile robots (Vertut and Coiffet, 1984 ; Kazerooni, 2005). Pneumatic systems provide a high degree of compliance and dexterity, high speed and force generation (Kazerooni, 2005). And therefore, cheap air supply is available everywhere in industrial surroundings (Shearer, 1956). But their principal drawback, the significant compressibility (*i.e.* sensitivity of volume to pressure) of air, unsettles their actuation quality (Shearer, 1956 ; Khayati et al., 2003). Moreover, varying thermodynamic states (temperature, density, *etc.*) cause an appreciable change in a number of the model's parameters. An accurate model plant of a standard pneumatic system must induce certain features, such as higher nonlinearities and varying thermodynamic parameters (Rifai and Bridges, 1997 ; Khayati et al., 2002a, 2003). In (Khayati et al., 2002b), the authors developed an effective pressure-controlled pneumatic system, employing a model that included 20 Hz to 100 Hz-frequency valve dynamics and nonlinear characteristics of the compressible flow through valve. Later, they proposed an effective procedure to develop a class of accurate models of pneumatic devices (Khayati et al., 2003). They addressed this issue by drawing up theoretical concepts (thermodynamics, fluid dynamics, *etc.*) under practical conditions (technological limitation, design, *etc.*).

More recently, these accurate models have been the subject of numerous papers on control strategies for pneumatic actuators. In (Khayati et al., 2002a), a robust pressure control scheme for a pneumatic servo system containing unknown possible nonlinear uncertainties was developed. Then, an implementation of a force control scheme was proposed (Khayati et al., 2004), which is described as a feedback linearization technique applied on the analytical nonlinear structure. Such a structure is dependently affine on parameter uncertainties, a generic characteristic of pneumatic plants. Moreover, parametric

uncertainties and exogenous disturbances arise on the deduced linear structure. Then, multi-objective constrained H_∞ and peak-to-peak gain minimizations were performed and compared.

In this contribution, a force controller is proposed for the fair *a priori* treatment of unbounded exogenous inputs in the context of the unperformed positioning control of a pneumatic actuator under friction. In practice, the friction force, which is unmeasurable, involves very complicated phenomena (non linearities and chaos) difficult to describe analytically and which rely on the physical properties of the contact surfaces (*e.g.* material properties, relative velocity and lubrication condition). And, generally, the friction does not produce an instantaneous response in the form of a change of velocity, *i.e.* it has internal dynamics; as stick-slip motion, pre-sliding displacement, Dahl effect and frictional lag (Armstrong-Helouvry et al., 1994). So, the classical friction models which are described by static mappings between the velocity and the friction force (as Coulomb friction and viscous friction models) remain unsatisfactory. Then, it was argued in (Armstrong-Helouvry et al., 1994) that dynamic models are necessary to describe friction phenomena accurately, and there are many of them in the Dahl model, the Bliman-Sorine model and the LuGre scheme (Canudas et al., 1995). The Dahl model offers a regularization of Coulomb friction at a velocity crossing zero, but this does not include stiction (Dahl, 1968). The LuGre and the Bliman-Sorine models can be regarded as extensions of the Dahl model to include stiction (Bliman and Sorine, 1995). However, the Bliman-Sorine model, which manifests oscillations in stick, cannot reproduce particular phenomena such as the Stribeck effect (*i.e.* the transient decrease in friction force from the stiction peak to the Coulomb level) and frictional lag (Gäfvert, 1997). These problems do not occur in the case of the LuGre model. For a review of some of these existing dynamic friction models, see *e.g.* (Armstrong-Helouvry et al., 1994) and references cited therein. Here, we assume that the friction phenomenon is of a dynamic nature, and is

covered by the LuGre friction model. Such a model captures most friction characteristics and is generically modeled as the average deflection force of elastic bristles between two contact surfaces. The bristles represent the asperities and irregularities characterizing the surfaces at a microscopic level.

Within this framework, we propose almost the same state-feedback linearization as given in (Khayati et al., 2004) to cancel most of nonlinearities. Then, the remaining system is investigated by a linear controller and a nonlinear action to attenuate the level of unbounded known inputs. As in (Khayati et al., 2002a, 2004), the synthesis of the linear controller gains is based on an appropriate closed-loop pole location, expressed in terms of linear matrix inequalities (LMIs). Finally, various experimental results are illustrated to validate the approach.

The present paper is organized as follows. In section 2, we describe the system we are considering and set forth our assumptions, which are accepted in practice to design pneumatic plants. Then, we introduce our model of the pneumatic actuator force dynamics, the motion control and friction compensation statement. Sections 3 and 4 describe respectively the force controller's components. A real-time implementation is presented in section 5 to elaborate various results and to illustrate the validity of our approach. Finally, concluding remarks are provided in section 6.

2 PNEUMATIC ACTUATOR MODELING

2.1 System description and assumptions

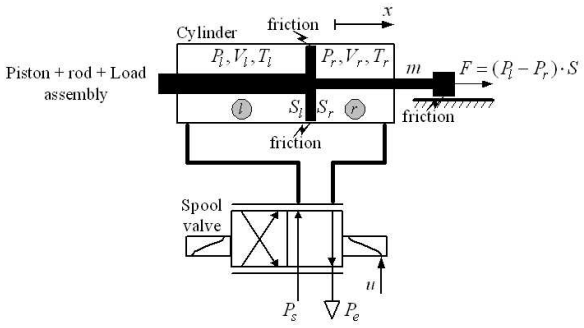

Figure 1. Pneumatic system scheme

The system we consider here (see Figure 1) consists of a rodless cylinder controlled with a current actuated servovalve. We assume that (Khayati et al., 2002a, 2003 ; Kazerooni, 2005):

- the gas is ideal;
- the air chamber's thermodynamic states (pressure, temperature, density) are uniform;
- the entire system's air temperature varies slightly from its nominal value;
- the turbulent flow process behaves somewhere between isothermally and adiabatically;
- the flow leakages are negligible;
- the motion of the $\{\text{piston} + \text{rod} + \text{load}\}$ assembly may be conducted under friction;

- the volume of each chamber and its instantaneous variations are easily measured time-varying characteristics;
- the pressure in each chamber is measured;
- the servovalve dynamics are negligible;
- the servovalve is characterized by an uncertain discharge coefficient.

2.2 Pressure force dynamics

Below, we propose a nonlinear affine control state-space model with structured uncertainties for the rate change of the inner pressures, in the left and the right chambers, based on the previous assumptions (Khayati et al., 2002a ; Kazerooni, 2005 ; Bigras, 2005), for $i = l, r$ and $o = e, s$ (see Figure 1):

$$\dot{P}_i = -\alpha(t) g_i(P_i, x, \dot{x}) + \beta(t) h_i(P_i, x, \mathrm{sgn}(u)) \cdot u$$

where

$$g_i(P_i, x, \dot{x}) = \frac{P_i \dot{V}_i(\dot{x})}{V_i(x)}$$

and

$$h_i(P_i, x, \mathrm{sgn}(u)) = \frac{\sqrt{RT_a}}{V_i(x)} W f(P_i) \mathrm{sgn}(u)$$

with

$$f(P_i) = \begin{cases} -P_i \bar{f}(\frac{P_o}{P_i}) \mid P_i > P_o \\ P_o \bar{f}(\frac{P_i}{P_o}) \mid P_i \leq P_o \end{cases}$$

where $\bar{f}$ designates the reduced flow function and is given by (Khayati et al., 2003 ; Kazerooni, 2005):

$$\bar{f}(p) = \begin{cases} C_1 & \text{if } p \leq p_{cr} \\ C_2 p^{\frac{1}{\zeta}} \sqrt{1 - p^{\frac{\zeta - 1}{\zeta}}} & \text{if } p > p_{cr} \end{cases}$$

with constants

$$C_1 = \sqrt{\frac{\zeta}{R}(\frac{2}{\zeta+1})^{\frac{\zeta+1}{\zeta-1}}}, C_2 = \sqrt{\frac{2\zeta}{R(\zeta-1)}} \text{ and } p_{cr} = (\frac{2}{\zeta+1})^{\frac{\zeta}{\zeta+1}}$$

P_l and P_r are the left and right chamber cylinder absolute pressures respectively. x and $\dot{x}$ are the cylinder piston position and velocity respectively. u corresponds to the valve spool position. P_e and P_s are the outer exhaust and supply absolute pressures respectively. T_a is the ambient absolute temperature. V_l and V_r are the left and right chamber volumes respectively. R is the universal gas constant. W is the spool constant. And, p_{cr} is the critical pressure ratio. $\alpha(\cdot)$ denotes the uncertain heat coefficient, which takes values between 1 and ζ, that is, the specific heat ratio and depends on the actual heat transfer occurring during the process (Khayati et al., 2003); $\beta(\cdot)$ is an uncertain parameter used to characterize the combination of the heat coefficient $\alpha(\cdot)$, the unknown valve discharge coefficient $C_d(\cdot)$ (Bigras, 2005) and the variation of the temperature $\tau(\cdot)$ (Khayati et al., 2003); and $\beta(\cdot)$ is generically expressed by (Khayati et al., 2003 ; Bigras, 2005):

$$\beta(t) = \alpha(t)C_d(t)\sqrt{\tau(t)}$$

We denote by S_l and S_r the piston cross-sectional areas of the left and right ports respectively. Then, the first-time derivative of the force produced by the actuator $F = P_l S_l - P_r S_r$ (see Figure 1) can be expressed as follows (Kazerooni, 2005):

$$\dot{F} = -\alpha(t)g(P_l, P_r, x, \dot{x}) + \beta(t)h(P_l, P_r, x, \text{sgn}(u))u \tag{2.1}$$

The functions $g(\cdot,\cdot,\cdot,\cdot)$ and $h(\cdot,\cdot,\cdot,\cdot)$ are found to be:

$$g(P_l, P_r, x, \dot{x}) = g_l(P_l, x, \dot{x}) \cdot S_l - g_r(P_r, x, \dot{x}) \cdot S_r \tag{2.2}$$

and

$$h(P_l, P_r, x, \text{sgn}(u)) = h_l(P_l, x, \text{sgn}(u)) \cdot S_l - h_r(P_r, x, \text{sgn}(u)) \cdot S_r \tag{2.3}$$

2.3 LuGre friction Model-based Piston-load dynamics

The dynamics of the cylinder motion under the influence of a dynamic friction f_{fr} and the actual pneumatic force F is given by:

$$m\ddot{x} = F - f_{fr} = P_l S_l - P_r S_r - f_{fr} \tag{2.4}$$

where m is the combined mass of piston, rod and load, and $\ddot{x}$ its acceleration. We model friction force variations f_{fr}, as follows (Canudas et al., 1995):

$$\dot{z} = -\frac{\sigma_0 |\dot{x}|}{\varphi(\dot{x})} z + \dot{x} \tag{2.5}$$

and

$$f_{fr} = \sigma_0 z + \sigma_1 \dot{z} + \sigma_2 \dot{x} \tag{2.6}$$

where the internal friction state z describes the average relative deflection of the bristle of the contact surfaces during the stiction phases. The parameter σ_0 is the stiffness of the bristle, σ_1 the frictional damping and σ_2 the viscous friction coefficient. The term $\varphi(\dot{x})$ is a finite function which can be chosen to describe different friction effects. One parameterization of $\varphi(\dot{x})$ to characterize the Stribeck effect is given in (Canudas et al., 1995):

$$\varphi(\dot{x}) = \mu_1 + (\mu_2 - \mu_1) \cdot e^{-\frac{\dot{x}^2}{\varsigma^2}} \tag{2.7}$$

The terms μ_1 and μ_2 correspond to the Coulomb friction and the stiction friction forces respectively. The parameter ς is the Stribeck relative velocity. It determines how $\varphi(\dot{x})$ may vary within its bounds μ_1 and μ_2.

All the dynamic and static friction parameters may vary due to the temperature changes, the relative velocity variation, the material wear, the lubrication condition and the normal acting forces between the contact surfaces (Canudas and Lischinsky, 1997 ; Madi et al., 2004). They are assumed to be uncertain, in some way, occasionally varying, but remain

always limited between lower and upper bounds, that is $\underline{\sigma}_j \leq \sigma_j \leq \overline{\sigma}_j$, for $j = 0, 1, 2$ and $\underline{\mu}_k \leq \mu_k \leq \overline{\mu}_k$, for $k = 1, 2$.

2.4 Motion controller and friction compensation statement

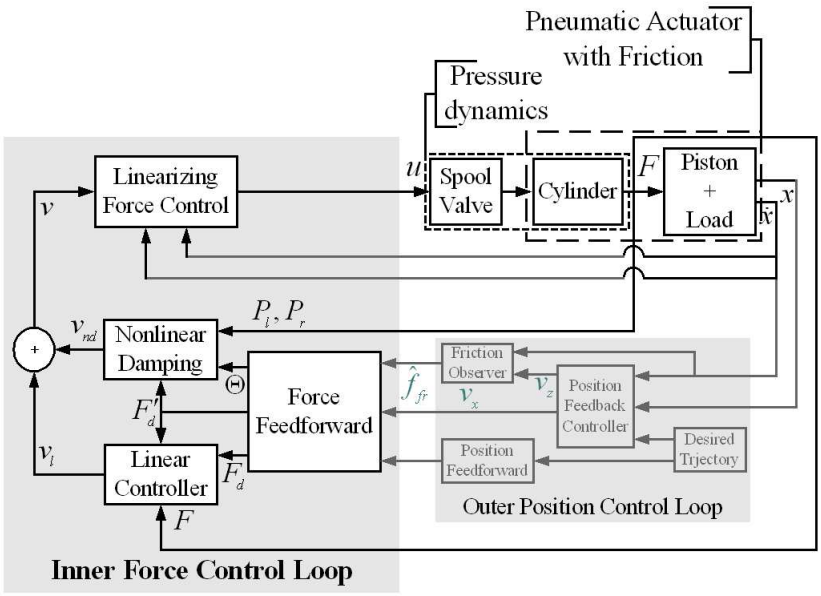

Figure 2. Proposed control strategy

The control objective is to design a controller to track any prescribed position trajectory under friction (see Figure 2), in accordance with a best tradeoff between stability proof and transient performances. Here, we take care to propose the friction compensation using nominal values of the friction coefficients, as follows:

$$\dot{\hat{z}} = -\frac{\sigma_{0n}|\dot{x}|}{\varphi_n(\dot{x})}\hat{z} + \dot{x} - v_z \tag{2.8}$$

and

$$\hat{f}_{fr} = \sigma_{0n}\hat{z} + \sigma_{1n}\dot{\hat{z}} + \sigma_{2n}\dot{x} \tag{2.9}$$

where

$$\varphi_n(\dot{x}) = \mu_{1n} + (\mu_{2n} - \mu_{1n}) \cdot e^{-\frac{\dot{x}^2}{\dot{x}_{sn}^2}} \tag{2.10}$$

v_z represents a deflection rate correction and constitutes any observer dynamic feedback term related to the measurable states of the position system.

3 FORCE CONTROLLER

In this section, we develop the force controller design using nonlinear plants to cancel most of the nonlinearities and unbounded known elements. A simple PI controller will be chosen to robustly stabilize the force error dynamics.

3.1 "Partial" linearization

We consider the pneumatic force dynamics (2.1). In order to efficiently apply a linear control law of the actuator output force F, we first propose the following feedback linearizing compensatory (Khayati et al., 2004):

$$u = \frac{v + \alpha_n g(P_l, P_r, x, \dot{x})}{\beta_n h(P_l, P_r, x, \mathrm{sgn}(u))} \tag{3.1}$$

where α_n is an 'additive' nominal value of α, that is, $\alpha = \alpha_n + \tilde{\alpha}$, and β_n is a 'multiplicative' value of β, that is, $\beta = \beta_n \cdot \tilde{\beta}$. So, we release system (2.1) of most known nonlinear dynamics by replacing (3.1) in (2.1):

$$\dot{F}(t) = \pi_1(t) g(P_l, P_r, x, \dot{x}) + \tilde{\beta}(t) v \tag{3.2}$$

where $\pi_1(t) = -\alpha(t) + \alpha_n \tilde{\beta}(t)$. The term $g(P_l, P_r, x, \dot{x})$, given by (2.2), is a function of known states: the pressure, which is bounded, the position, and particularly the velocity, which are not bounded *a priori*. So, the use of any optimization criterion, as in (Khayati et al., 2004), is not appropriate here, and the force dynamics (3.2) cannot be treated only by using a linear compensator. Below, we complete the design of the force controller, which yields a sufficient condition toward the position loop investigation.

3.2 PI + nonlinear damping compensators

The control objective is for the actuator output force F to track a specific time-varying force $F_d(t)$ encountering the position problem under friction. $F_d(t)$ is described by:

$$F_d(t) = m\ddot{x}_d + \hat{f}_{fr} + v_x \tag{3.3}$$

$\ddot{x}_d$ is the twice derivative of the sufficiently smooth tracking reference x_d. v_x designates any controller action related to the measurable states of the position system. Let $\tilde{F}$ be the tracking error, that is

$$\tilde{F} = F - F_d \tag{3.4}$$

Let $\mathbf{X} = \begin{pmatrix} \int \tilde{F}dt & \tilde{F} \end{pmatrix}^{\mathrm{T}}$ be the vector of force error states. The tracking system model for the pneumatic force is derived as:

$$\dot{\mathbf{X}} = \mathbf{A}\mathbf{X} + \mathbf{B} \cdot (\tilde{\beta}(t)v + \pi_1(t)g(P_l, P_r, x, \dot{x}) - \dot{F}_d(t, \dot{x})) \tag{3.5}$$

with

$$\mathbf{A} = \begin{pmatrix} 0 & 1 \\ 0 & 0 \end{pmatrix} \text{ and } \mathbf{B} = \begin{pmatrix} 0 \\ 1 \end{pmatrix}$$

In particular, in accordance with the modelization of the friction force (2.5)-(2.7) and its estimate (2.8)-(2.10), we can write the tracking reference differentiation $\dot{F}_d(t, \dot{x})$ as a combination of continuous and discontinuous terms, as follows:

$$\dot{F}_d(t, \dot{x}) = F'_d(t, \dot{x}) - \pi_2(t)\Theta(t, \dot{x}) \tag{3.6}$$

with

$$\Theta(t, \dot{x}) = \frac{\sigma_{0n}\sigma_{1n}}{\varphi_n(\dot{x})}\hat{z}\ddot{x} \tag{3.7}$$

and

$$\pi_2(t) = \mathrm{sgn}(\dot{x}) - \mathrm{sat}(\dot{x}) \tag{3.8}$$

Remark 3.1. On differentiating the tracking reference $F_d(t)$, given in (3.3), the term $\dot{\hat{f}}_{fr}$ is not rather continuous, as it contains the term $\frac{\sigma_{0n}\sigma_{1n}}{\varphi_n(\dot{x})}\hat{z}\ddot{x}\mathrm{sgn}(\dot{x})$. Then, we replace the function $\mathrm{sgn}(\dot{x})$ by $\mathrm{sat}(\dot{x})$ which is continuous. Below, we will replace (3.6) in (3.5).

Remark 3.2. $F_d'(t,\dot{x})$ denotes a continuous approximation of the tracking reference derivative, and $\pi_2(t)\Theta(t,\dot{x})$ its approximation error. $\Theta(t,\dot{x})$ is a continuous function and $\pi_2(t)$ is an uncertain parameter, and includes the discontinuity feature around zero velocity. The following controller design is based on the well-known nonlinear damping approach (Khalil, 2002), which is robustly applied within a multiplicative uncertainty component (the term $\tilde{\beta}(t)$ in (3.5)).

Proposition 3.1. Consider system (3.2). If the control action v is finely defined as a linear combination of two terms (see Figure 2):

$$v = v_l + v_{nd} \tag{3.9}$$

where

$$v_l = F_d'(t,\dot{x}) - \mathbf{KX} \tag{3.10}$$

and

$$v_{nd} = -\frac{\kappa}{\underline{\tilde{\beta}}}(g(P_l,P_r,x,\dot{x})^2 + F_d'(t,\dot{x})^2 + \Theta(t,\dot{x})^2)\mathbf{B}^{\mathrm{T}}\mathbf{P}^{-1}\mathbf{X} \tag{3.11}$$

with $\underline{\tilde{\beta}}$ is the lower bound of the uncertain parameter $\tilde{\beta}(t)$. Then the closed-loop system is uniformly bounded. v_l is the term that is linearly dependent on the errors and the continuous feed-forward term $F_d'(t,\dot{x})$ and v_{nd} is the nonlinear damping term, but smoothed action to compensate for exogenous inputs of the closed-loop force dynamics. Moreover, the state-feedback $\mathbf{KX}$ is introduced such that there exists a unique positive definite and symmetrical matrix $\mathbf{P}$ for a given positive definite and symmetrical $\mathbf{Q}_{\tilde{\beta}}$ to the Lyapunov equations:

$$(\mathbf{A} - \tilde{\beta}(t)\mathbf{BK})\mathbf{P} + \mathbf{P}(\mathbf{A} - \tilde{\beta}(t)\mathbf{BK})^{\mathrm{T}} + \mathbf{Q}_{\tilde{\beta}} = 0 \tag{3.12}$$

for any $\tilde{\beta}(t) \in [\underline{\tilde{\beta}}, \overline{\tilde{\beta}}]$. Finally, we choose $\kappa > 0$.

Proof. The substitution of (3.6) and (3.9), and then (3.10), into (3.5) yields the following state error dynamics:

$$\dot{\mathbf{X}} = (\mathbf{A} - \tilde{\beta}(t)\mathbf{B}\mathbf{K})\mathbf{X} + \mathbf{B}(\tilde{\beta}(t)v_{nd} + \pi_1(t)g(P_l, P_r, x, \dot{x}) + \pi_2(t)\Theta(t, \dot{x}) + \pi_3(t)F_d'(t, \dot{x}))$$

with $\pi_3(t) = \tilde{\beta}(t) - 1$.

Choose the Lyapunov function candidate for this system as $V = \frac{1}{2}\mathbf{X}^{\mathrm{T}}\mathbf{P}^{-1}\mathbf{X}$. Then, the time derivative of V along the solution of the system will be

$$\begin{aligned}
\dot{V} = \; & \tfrac{1}{2}\mathbf{X}^{\mathrm{T}}[\mathbf{P}^{-1}(\mathbf{A} - \tilde{\beta}(t)\mathbf{B}\mathbf{K}) + (\mathbf{A} - \tilde{\beta}(t)\mathbf{B}\mathbf{K})^{\mathrm{T}}\mathbf{P}^{-1}]\mathbf{X} + \mathbf{X}^{\mathrm{T}}\mathbf{P}^{-1}\mathbf{B}(\tilde{\beta}(t)v_{nd} + \\
& \pi_1(t)g(P_l, P_r, x, \dot{x}) + \pi_2(t)\Theta(t, \dot{x}) + \pi_3(t)F_d'(t, \dot{x})) \\
\leq \; & -\tfrac{1}{2}\mathbf{X}^{\mathrm{T}}\mathbf{P}^{-1}\mathbf{Q}_{\tilde{\beta}}\mathbf{P}^{-1}\mathbf{X} + \mathbf{X}^{\mathrm{T}}\mathbf{P}^{-1}\mathbf{B}\tilde{\beta}(t)v_{nd} + \bar{\pi}_1|\mathbf{X}^{\mathrm{T}}\mathbf{P}^{-1}\mathbf{B}g(P_l, P_r, x, \dot{x})| + \\
& \bar{\pi}_2|\mathbf{X}^{\mathrm{T}}\mathbf{P}^{-1}\mathbf{B}\Theta(t, \dot{x})| + \bar{\pi}_3|\mathbf{X}^{\mathrm{T}}\mathbf{P}^{-1}\mathbf{B}F_d'(t, \dot{x})|
\end{aligned}$$

with $\bar{\pi}_1 = \max(|\pi_1|) > |\pi_1|$, $\bar{\pi}_2 = \max(|\pi_2|) > |\pi_2|$ and $\bar{\pi}_3 = \max(|\pi_3|) > |\pi_3|$. Next, define

$$v_{nd} = -\frac{1}{\underline{\tilde{\beta}}}(\kappa_1 g(P_l, P_r, x, \dot{x})^2 + \kappa_2\Theta(t, \dot{x})^2 + \kappa_3 F_d'(t, \dot{x})^2)\mathbf{B}^{\mathrm{T}}\mathbf{P}^{-1}\mathbf{X} \tag{3.13}$$

Then, we have

$$\begin{aligned}
\dot{V} \leq \; & -\tfrac{1}{2}\mathbf{X}^{\mathrm{T}}\mathbf{P}^{-1}\mathbf{Q}_{\tilde{\beta}}\mathbf{P}^{-1}\mathbf{X} - \kappa_1|\mathbf{B}^{\mathrm{T}}\mathbf{P}^{-1}\mathbf{X}|^2|g(P_l, P_r, x, \dot{x})|^2 + \bar{\pi}_1|\mathbf{B}^{\mathrm{T}}\mathbf{P}^{-1}\mathbf{X}|\cdot \\
& |g(P_l, P_r, x, \dot{x})| - \kappa_2|\mathbf{B}^{\mathrm{T}}\mathbf{P}^{-1}\mathbf{X}|^2|\Theta(t, \dot{x})|^2 + \bar{\pi}_2|\mathbf{B}^{\mathrm{T}}\mathbf{P}^{-1}\mathbf{X}||\Theta(t, \dot{x})| \\
& - \kappa_3|\mathbf{B}^{\mathrm{T}}\mathbf{P}^{-1}\mathbf{X}|^2|F_d'(t, \dot{x})|^2 + \bar{\pi}_3|\mathbf{B}^{\mathrm{T}}\mathbf{P}^{-1}\mathbf{X}||F_d'(t, \dot{x})|
\end{aligned}$$

The term $-\kappa_1|\mathbf{B}^{\mathrm{T}}\mathbf{P}^{-1}\mathbf{X}|^2|g(P_l, P_r, x, \dot{x})|^2 + \bar{\pi}_1|\mathbf{B}^{\mathrm{T}}\mathbf{P}^{-1}\mathbf{X}||g(P_l, P_r, x, \dot{x})|$ has a maximum of $\frac{\bar{\pi}_1^2}{4\kappa_1}$ at $|\mathbf{B}^{\mathrm{T}}\mathbf{P}^{-1}\mathbf{X}|\ |g(P_l, P_r, x, \dot{x})| = \frac{\bar{\pi}_1}{2\kappa_1}$. The term $-\kappa_2|\mathbf{B}^{\mathrm{T}}\mathbf{P}^{-1}\mathbf{X}|^2|\Theta(t, \dot{x})|^2 + \bar{\pi}_2|\mathbf{B}^{\mathrm{T}}\mathbf{P}^{-1}\mathbf{X}||\Theta(t, \dot{x})|$ has a maximum of $\frac{\bar{\pi}_2^2}{4\kappa_2}$ at $|\mathbf{B}^{\mathrm{T}}\mathbf{P}^{-1}\mathbf{X}||\Theta(t, \dot{x})| = \frac{\bar{\pi}_2}{2\kappa_2}$. And, finally, the term $-\kappa_3|\mathbf{B}^{\mathrm{T}}\mathbf{P}^{-1}\mathbf{X}|^2|F_d'(t, \dot{x})|^2 + \bar{\pi}_3|\mathbf{B}^{\mathrm{T}}\mathbf{P}^{-1}\mathbf{X}||F_d'(t, \dot{x})|$ has a maximum of $\frac{\bar{\pi}_3^2}{4\kappa_3}$ at $|\mathbf{B}^{\mathrm{T}}\mathbf{P}^{-1}\mathbf{X}|$

$|F'_d(t,\dot{x})| = \frac{\bar{\pi}_3}{2\kappa_3}$, then

$$\dot{V} \leq -\frac{1}{2}\mathbf{X}^{\mathrm{T}}\mathbf{P}^{-1}\mathbf{Q}_{\tilde{\beta}}\mathbf{P}^{-1}\mathbf{X} + \frac{\bar{\pi}_1^2}{4\kappa_1} + \frac{\bar{\pi}_2^2}{4\kappa_2} + \frac{\bar{\pi}_3^2}{4\kappa_3}$$

$\dot{V}$ is negative outside some ball (see lemma 14.1 in (Khalil, 2002)). It follows from Theorem 4.18 in (Khalil, 2002) that, for any initial state $\mathbf{X}(t_0)$, the solution of the closed-loop system is uniformly bounded. Finally, we choose $\kappa = \max(\kappa_1, \kappa_2, \kappa_3)$. ■

4 PI GAINS SYNTHESIS

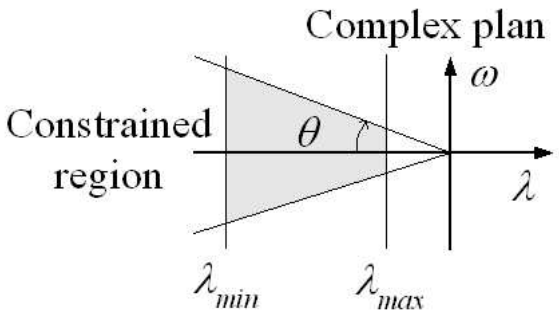

Figure 3. Stability region $\mathcal{D}$

The model of the closed-loop system, given by (3.5) and (3.9)-(3.11), represents an affine parameter-dependent system (PDS) with respect to the parameter uncertainty $\tilde{\beta}$. According to the proposition result given above, for any vector gain $\mathbf{K}$ respecting (3.12), the linear part of this PDS feature is uniformly asymptotically stable. Moreover, this item can be numerically solved by using LMI frameworks. In addition, for a robust synthesis, which takes into account the structured bounded uncertainties (Chilali et al., 1999), the linear part of this PDS can have a specific decay rate and maximum possible damping in all modes and can prevent fast controller dynamics. That being so, the multi-objective controller design will be formulated as a pole clustering feasibility problem in a $\mathcal{D}$-stability region involving LMIs. Thereafter, the closed-loop stability condition (3.12) will be replaced by the $\mathcal{D}$-stability (see Figure 3) given by (Chilali and Gahinet, 1996 ; Chilali et al., 1999):

$$\mathcal{D}(\lambda_{min}, \lambda_{max}, \theta) \triangleq \{\lambda + j\omega \in \mathbb{C} \mid \lambda_{min} \leq \lambda \leq \lambda_{max};\ \tan\theta \cdot \sigma < -|\omega|\} \tag{4.1}$$

for chosen λ_{min}, λ_{max} and θ. Meanwhile, confining the closed loop poles to this subregion bounds the settling time, the frequency of oscillatory modes and the maximum overshoot

respectively. Firstly, denote by $\mathcal{L}^+$ and $\mathcal{L}^-$ the following matricial operators:

$$\mathcal{L}^+(\mathtt{X}_1, \mathtt{Y}_1, \mathtt{X}_2, \mathtt{Y}_2) = (\mathtt{X}_1\mathtt{Y}_1 + \mathtt{Y}_1'\mathtt{X}_1') - (\mathtt{X}_2\mathtt{Y}_2 + \mathtt{Y}_2'\mathtt{X}_2')$$

and

$$\mathcal{L}^-(\mathtt{X}_1, \mathtt{Y}_1, \mathtt{X}_2, \mathtt{Y}_2) = (\mathtt{X}_1\mathtt{Y}_1 - \mathtt{Y}_1'\mathtt{X}_1') - (\mathtt{X}_2\mathtt{Y}_2 - \mathtt{Y}_2'\mathtt{X}_2')$$

By using the LMI-regions (Chilali and Gahinet, 1996), the $\mathcal{D}$-stability of the linear part of the error force dynamics can be reduced to the following matrix inequality statements: $\forall \tilde{\beta} \in [\underline{\tilde{\beta}}, \overline{\tilde{\beta}}]$,

$$\mathbf{P} > 0 \tag{4.2}$$

$$\mathcal{L}^+(\mathbf{A}, \mathbf{P}, \tilde{\beta}\mathbf{B}\mathbf{K}, \mathbf{P}) - 2\lambda_{min}\mathbf{P} > 0 \tag{4.3}$$

$$\mathcal{L}^+(\mathbf{A}, \mathbf{P}, \tilde{\beta}\mathbf{B}\mathbf{K}, \mathbf{P}) - 2\lambda_{max}\mathbf{P} < 0 \tag{4.4}$$

and

$$\begin{bmatrix} \sin\theta \cdot \mathcal{L}^+(\mathbf{A}, \mathbf{P}, \tilde{\beta}\mathbf{B}\mathbf{K}, \mathbf{P}) & \cos\theta \cdot \mathcal{L}^-(\mathbf{A}, \mathbf{P}, \tilde{\beta}\mathbf{B}\mathbf{K}, \mathbf{P}) \\ -\cos\theta \cdot \mathcal{L}^-(\mathbf{A}, \mathbf{P}, \tilde{\beta}\mathbf{B}\mathbf{K}, \mathbf{P}) & \sin\theta \cdot \mathcal{L}^+(\mathbf{A}, \mathbf{P}, \tilde{\beta}\mathbf{B}\mathbf{K}, \mathbf{P}) \end{bmatrix} < 0 \tag{4.5}$$

the variables of which are the symmetrical Lyapunov matrix $\mathbf{P}$ and the gain matrix $\mathbf{K}$ respectively.

Since expressions in (4.2)-(4.5) involve nonlinear terms of the form $\mathbf{BKP}$, the resulting feasibility problem is nonlinear. However the LMI formulation is readily restored by rewriting (4.2)-(4.5) in terms of $\mathbf{P}$ and the auxiliary variable $\mathbf{W} = \mathbf{KP}$ (Boyd et al., 1994). The given LMIs are, in fact, used to be affine in variables $\mathbf{P}$ and $\mathbf{W}$. Now, observe that the closed-loop system is an affine PDS with respect to $\tilde{\beta}$ which is included in the convex set $[\underline{\tilde{\beta}}, \overline{\tilde{\beta}}]$. That being so, the LMIs are given equivalently by the following: for $k = 1, 2$;

$$\mathbf{P} > 0 \tag{4.6}$$

$$\mathcal{L}_k^+ - 2\lambda_{min}\mathbf{P} > 0 \tag{4.7}$$

$$\mathcal{L}_k^+ - 2\lambda_{max}\mathbf{P} < 0 \tag{4.8}$$

$$\begin{bmatrix} \sin\theta \cdot \mathcal{L}_k^+ & \cos\theta \cdot \mathcal{L}_k^- \\ -\cos\theta \cdot \mathcal{L}_k^- & \sin\theta \cdot \mathcal{L}_k^+ \end{bmatrix} < 0 \tag{4.9}$$

where

$$\mathcal{L}_1^+ = \mathcal{L}^+(\mathbf{A}, \mathbf{P}, \underline{\tilde{\beta}}\mathbf{B}, \mathbf{W})\,; \quad \mathcal{L}_1^- = \mathcal{L}^-(\mathbf{A}, \mathbf{P}, \underline{\tilde{\beta}}\mathbf{B}, \mathbf{W})$$
$$\mathcal{L}_2^+ = \mathcal{L}^+(\mathbf{A}, \mathbf{P}, \overline{\tilde{\beta}}\mathbf{B}, \mathbf{W})\,; \quad \mathcal{L}_2^- = \mathcal{L}^-(\mathbf{A}, \mathbf{P}, \overline{\tilde{\beta}}\mathbf{B}, \mathbf{W})$$

5 EXPERIMENTAL RESULTS

Table I. Numerical values

Parameter	Lower value	Upper value	Nominal value
m (kg)	-	-	0.326
u_{max} (m)	-	-	0.002
P_e (kPa)	-	-	101.
P_s (kPa)	-	-	608.
R (N $\cdot$ m/kg $\cdot$ K)	-	-	287.
$S_l = S_r$ (m^2)	-	-	$4.9\ 10^{-4}$
T_a (K)	-	-	295.
$V_{c_{max}}$ (m^3)	-	-	$2.45\ 10^{-4}$
W (m)	-	-	0.005
α	1.0	1.3997	1.1999
β	0.075	1.3297	0.7023
ζ	-	-	1.4
μ_1 (N)	30.	38.	34.
μ_2 (N)	50.	55.	52.5
σ_0 (N/m)	$1.0159\ 10^5$	$1.6506\ 10^5$	$1.3780\ 10^5$
σ_1 (N $\cdot$ s/m)	0.	140.6	70.3
σ_2 (N $\cdot$ s/m)	119.9	220.1	170.0
ς (m/s)	10^{-3}	10^{-1}	0.05

The effectiveness of the proposed force control is illustrated by results of implementation of an experimental setup. The performances are depicted within two different contexts:

using position open-loop and closed-loop controls. The experimental system consists of a rodless cylinder (FESTO, DGP-25-500) controlled with a current actuated servovalve (FESTO, MPYE-5-1/8LF-010B). The air supply is tuned via a regulator model (FESTO, LFR-M2-G1/4-C10RG). Pressure sensors (FESTO, SDE-10) are used to measure the pressure drop. The piston displacement is measured with a position sensor (FESTO, MLD-POT-500-TLF). The spool valve displacement and the sensor measurements are respectively sent and received through an acquisition card (PCI-6052E). The velocity and acceleration are obtained by differentiating and digitally filtering the position measurements. The control algorithms are implemented using XPC-Simulink software and the MATLAB© Real-Time-Workshop, with a sampling period of 100μs.

The system parameters are given in Table I. To ensure the $\mathcal{D}$-stability of the uncertain linear part of the system, we choose the following stability region bounds: $\lambda_{min} = -120$, $\lambda_{max} = -2$ and $\theta = \arccos 0.7$. This is a compromise between the settling time of the response, the frequency of the oscillatory modes, the non-saturation of the control effort and the maximum overshoot. The LMIs (4.6)-(4.9) have been implemented using LMI Toolbox the MATLAB© (Gahinet et al., 1995). We obtain the following linear controller gains: $\mathbf{K} = [177.8\ ;\ 74.9]$.

To investigate the performance of the proposed control using a position open-loop, the force control problem is to apply different shapes of the desired force trajectory. Figures (4-a), (5-a) and (6-a) show the actual and desired forces of three different force reference trajectories. The error remains ultimately bounded. On the other hand, the corresponding control efforts displayed in Figures (4-b), (5-b) and (6-b) show that the spool valve does not exceed the maximum voltage of 10 Volts (which is equivalent to the maximum spool position u_{max}). Finally, Figures (4-c), (4-d), (5-c), (6-d), (5-c) and (6-d) show the pressure levels in each chamber of the cylinder.

Thereafter, we propose to seek for the controller performance when using a position closed-loop control under friction, according to the context of the subsection 3.4 given above. In Figure 7, we show the position and force performances when tracking a $0.25\ \mathrm{Hz}$ sine position input with amplitude of $30\ \mathrm{mm}$. Moreover, these performances are investigated, in the case of an other smooth input to cross a distance of $80\ \mathrm{mm}$, and given in Figure 8. Finally, the corresponding input voltages and chamber pressures are also depicted.

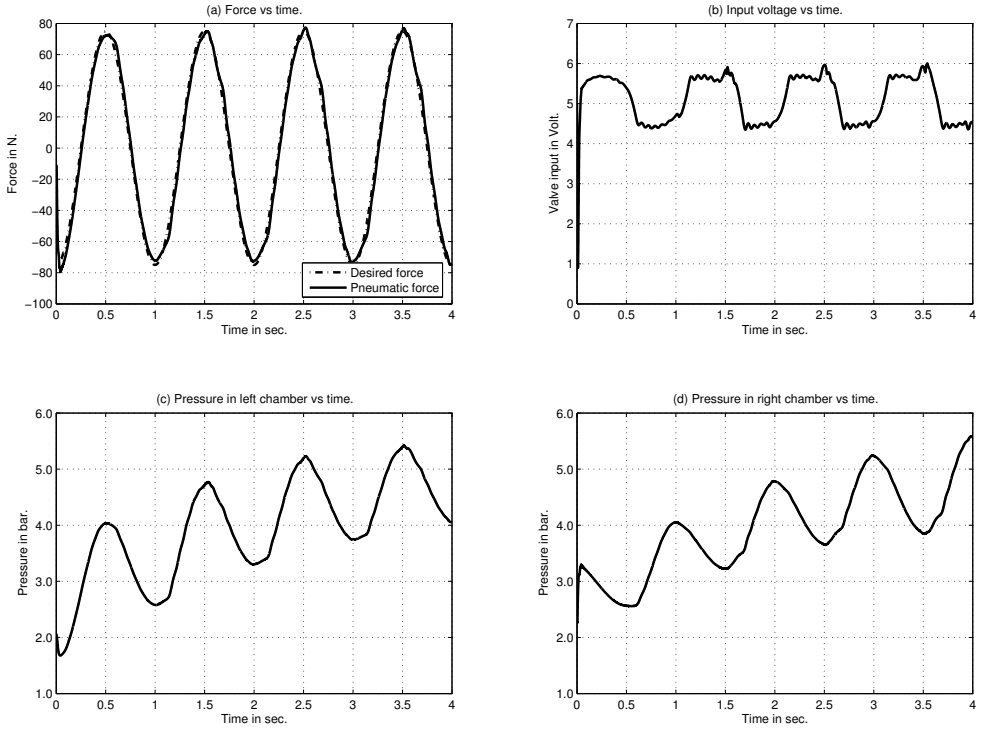

Figure 4. Force control performance for a sine-force reference (using only the inner loop)

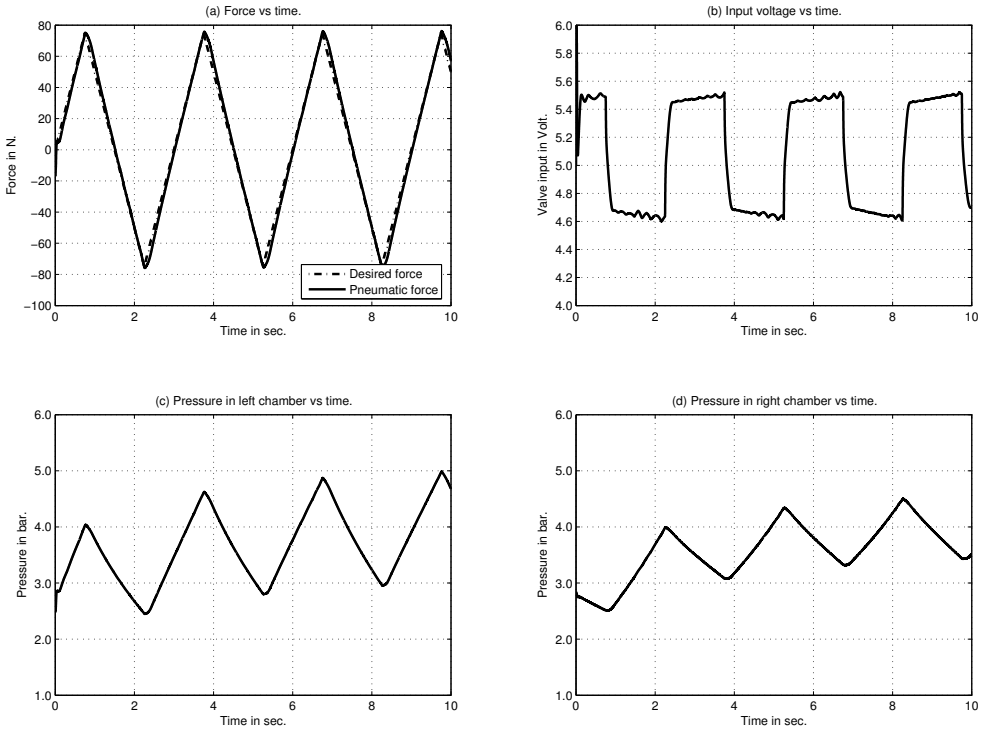

Figure 5. Force control performance for a triangle-force reference (using only the inner loop)

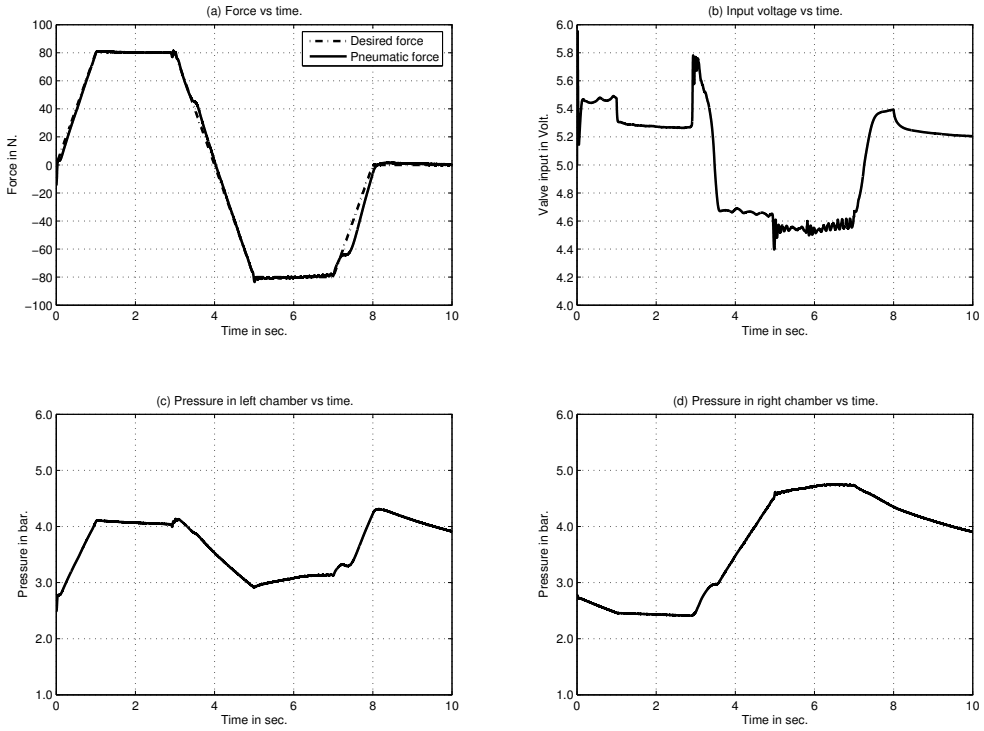

Figure 6. Force control performance for a tooth-force reference (using only the inner loop)

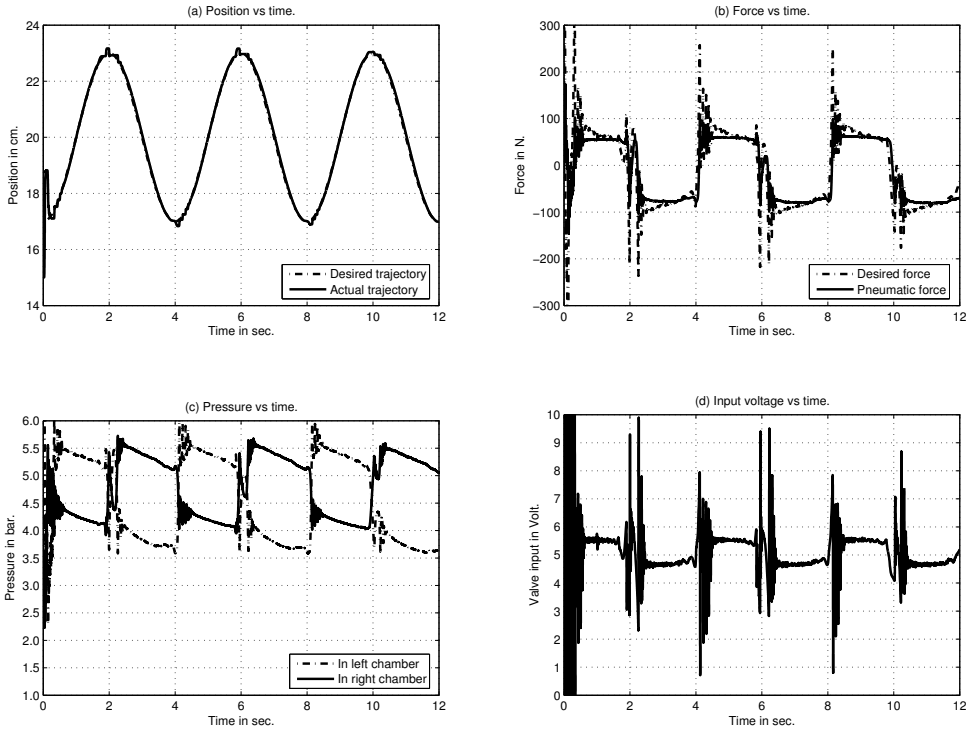

Figure 7. Force control performance for a sine-position reference (using both the inner and outer loops)

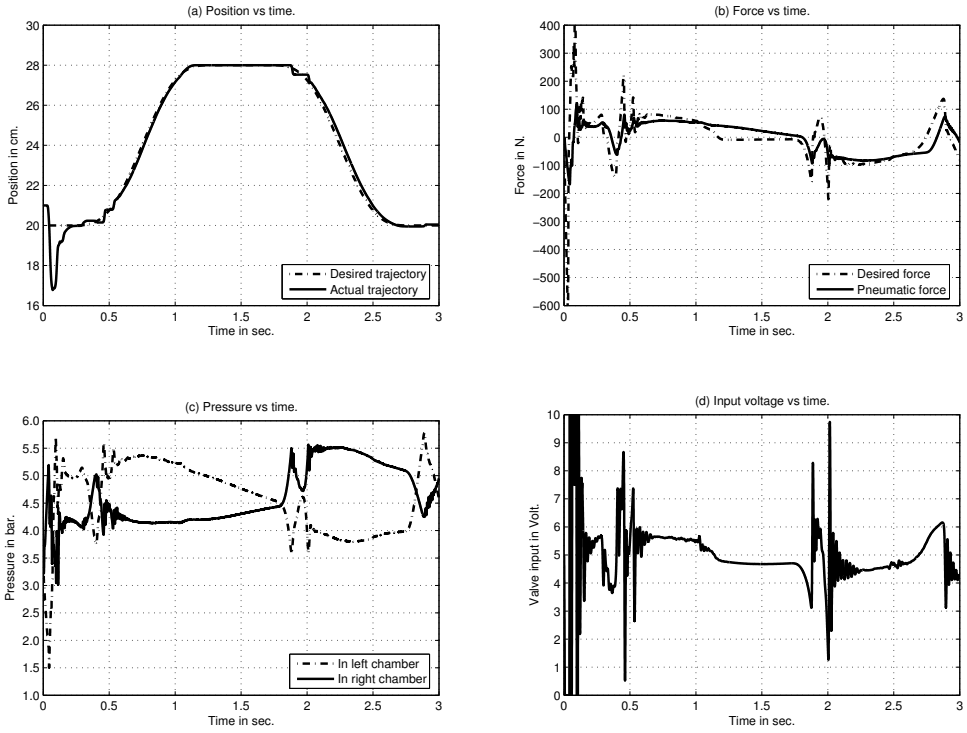

Figure 8. Force control performance for a linear-quadratic-position reference (using both the inner and outer loops)

6 CONCLUSION

In this paper, we have proposed a complete design of a pneumatic actuator force control, taking into account parameter uncertainty and the scheme's possible unbounded aspects. The proposed scheme is suitable for immediate use to address the problem of the piston motion control under friction. It is composed of a state-feedback linearization, to cancel most of the known nonlinearities, a robust linear state-feedback and another nonlinear compensator to ultimately render the force error bounded. To this end, a detailed proof is established, and experimental results are presented. The force performance shown is sufficient to robustly compensate for motion driving under friction.

REFERENCES

Armstrong-Helouvry, B., Dupont, P., Canudas, C. (1994). A Survey of Models, Analysis Tools and Compensation Methods for the Control of Machines with Friction. *Automatica*, 30(7):1083–1138.

Bigras, P. (2005). Sliding-Mode Observer as a Time-Variant Estimator for Control of Pneumatic Systems. *Journal of Dynamic Systems, Measurement and Control, Trans. of the ASME*, 127:499–502.

Bliman, P.-A., Sorine, M. (1995). Easy-To-Use Realistic Dry Friction Models for automatic Control. In *Proc. of the European Contr. Conf.*, pp. 3788–3794, Rome, Italy.

Boyd, S., El-Ghaoui, L., Feron, E., Balakrishnan, V. (1994). *Linear Matrix Inequalities in Systems and Control Theory*, Volume 15 of *SIAM Studies in Applied Mathematics*. Society for Industrial and Applied Mathematics, Philadelphia, PA.

Canudas, C., Lischinsky, P. (1997). Adaptive Friction Compensation with a Partially Known Dynamic Friction Model. *Int. J. of Adaptive Contr. and Signal Processing*, 11:65–80.

Canudas, C., Olsson, H., Aström, K., Lischinsky, P. (1995). A New Model for Control of Systems with Friction. *IEEE Trans. Automat. Contr.*, 40(3):419–425.

Chilali, M., Gahinet, P. (1996). H_∞ Design with Pole Placement Constraints: An LMI Approach. *IEEE Trans. Automat. Contr.*, 41(3):358–367.

Chilali, M., Gahinet, P., Apkarian, P. (1999). Robust Pole Placement in LMI Regions. *IEEE Trans. Automat. Contr.*, 44(12):2257–2270.

Dahl, P. (1968). A Solid Friction Model. Technical Report TOR-158, The Aerospace Corporation, CA.

Gäfvert, M. (1997). Comparisons of Two Dynamic Friction Models. In *Proc. of the IEEE Int. Conf. on Control Applications*, pp. 386–391, Hartford.

Gahinet, P., Nemirovskii, A., Laub, A., Chilali, M. (1995). *MATLAB LMI Control Toolbox*. The MathWorks Inc., MA.

Kain, J., Wartelle, C. (1973). *Dynamique des vérins pneumatiques*. Les mémoires techniques du CETIM.

Kazerooni, H. (2005). Design and Analysis of Pneumatic Force Generators for Mobile Robotic Systems. *IEEE/ASME Trans. Mechatronics*, 10(4):411–418.

Khalil, H. (2002). *Nonlinear Systems*. Prentice-Hall, New York.

Khayati, K., Bigras, P., Dessaint, L.-A. (2002a). A Robust Pole Clustering Design of Pneumatic Systems using LMI Approach. In *Proc. of the IEEE Int. Conf. on Systems, Man and Cybernetics*, Volume 4, pp. 274–279, Hammamet, Tunisia.

Khayati, K., Bigras, P., Dessaint, L.-A. (2002b). Retaining or Neglecting Valve Spool Dynamics in Tracking Controller Strategies for Pneumatic Systems. In *Proc. of the IEEE Int. Conf. on Methods and Models in Automation and Robotics*, pp. 1213–1218, Szczecin, Poland.

Khayati, K., Bigras, P., Dessaint, L.-A. (2003). On Modelization and Robust Controller Synthesis of Pneumatic Actuator Plants using LMI Approach. In *Proc. of the CESA*, S1-R-00-0304, Lille, France.

Khayati, K., Bigras, P., Dessaint, L.-A. (2004). A Robust Feedback Linearization Force Control of a Pneumatic Actuator. In *Proc. of the IEEE Int. Conf. on Systems, Man and Cybernetics*, pp. 6113–6119, The Hague, Holland.

Lai, J., Menq, C.-H., Singh, R. (1989). Pressure Control of a Pneumatic Chamber. *Journal of Fluid Control*, 19(4):7–31.

Madi, M., Khayati, K., Bigras, P. (2004). Parameter Estimation for the LuGre Friction Model using Interval Aanalysis and Set Inversion. In *Proc. of the IEEE Int. Conf. on Systems, Man and Cybernetics*, pp. 428–433, The Hague, Holland.

Mc Cloy, D., Martin, H. (1973). *The Control of Fluid Power*. Longman, London.

Richer, E., Hurmuzlu, Y. (2000). High Performance Pneumatic Force Actuator System: Part I- Nonlinear Mathematical Model. *Journal of Dynamic Systems, Measurement and Control, Transactions of the ASME*, 122(3):416–425.

Rifai, O., Bridges, M. (1997). Integrator Backstepping Control Of A Pneumatic Actuator-Based Robot Manipulator. In *Proc. of the ASME, Dynamic Systems and Control Division*, pp. 487–495.

Scherer, C., Gahinet, P., Chilali, M. (1997). Multiobjective Output-Feedback Control via LMI Optimization. *Automatic Control IEEE Trans.*, 42(7):896–911.

Shearer, J. (1956). Study of Pneumatic Processes in the Continuous Control of Motion with Compressed Air - I, II. *Trans. of the ASME*, 122(3):233–249.

Vertut, J., Coiffet, P. (1984). *Les Robots - Téléopération: Évolution des Technologies - Tome 3*. Hermes Publishing, Paris.